Substituent Effects in CH Hydrogen Bond Interactions: Linear Free Energy Relationships and Influence of Anions

Blakely W. Tresca,[†] Ryan J. Hansen,[†] Calvin V. Chau,[†] Benjamin P. Hay,[‡] Lev N. Zakharov,[§] Michael M. Haley,*,[†] and Darren W. Johnson*,[†]

[†]Department of Chemistry & Biochemistry and the Materials Science Institute, University of Oregon, Eugene, Oregon 97403-1253, United States

[‡]Supramolecular Design Institute, 127 Chestnut Hill Road, Oak Ridge, Tennessee 37830-7185, United States

[§]CAMCOR, University of Oregon, 1443 East 13th Avenue, Eugene, Oregon 97403, United States

S *Supporting Information*

ABSTRACT: Aryl CH hydrogen bonds (HBs) are now commonly recognized as important factors in a number of fields, including molecular biology, stereoselective catalysis, and anion supramolecular chemistry. As the utility of CH HBs has grown, so to has the need to understand the structure–activity relationship for tuning both their strength and selectivity. Although there has been significant computational effort in this area, an experimental study of the substituent effects on CH HBs has not been previously undertaken. Herein we disclose a systematic study of a single CH HB by using traditional urea donors as directing groups in a supramolecular binding cavity. Experimentally determined association constants are examined

by a combination of computational (electrostatic potential) and empirical (σ_m and σ_p) values for substituent effects. The dominance of electrostatic parameters, as observed in a computational DFT study, is consistent with current CH HB theory; however, a novel anion dependence of the substituent effects is revealed in solution.
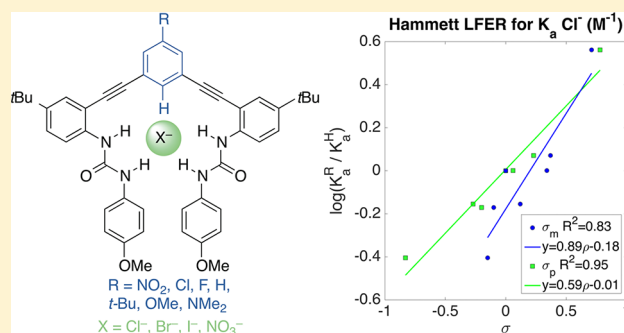
INTRODUCTION

CH hydrogen bonds (HBs) are now understood to be a ubiquitous structural feature in chemistry and biology.[1,2] CH donors play important and previously unrecognized roles in the multidisciplinary fields of molecular biology, supramolecular chemistry,[3–5] and catalysis.[1,6] CH···O HBs are common in protein folding and are found in the minor groove of DNA.[7,8] Catalysts have also been found to include CH···O HBs as an important factor in stereoselectivity.[6] Chemists are now widely using CH groups as HB donors in designed systems for anion capture[1,9–11] and catalysis.[12,13]

New CH donors have been developed to maximize the strength of a CH HB, including triazoles, bisketo-boronates, and pyridinium ions (Figure 1a).[14] These strong, acidic CH donors, when incorporated within heterocycles with electron-poor atoms, are aligned to maximize the C←H dipole. The development of such new CH donors has increased the utility of these nonclassical HBs in structural design.

Despite the numerous computational studies on strong CH HB donors, experimental studies that quantify the energetic components of CH HBs, especially for weaker donors like benzene, have proven very difficult to obtain. As such, explanations and descriptions for CH HB strengths have been overwhelmingly dominated by the electrostatic component. Notable computational and experimental studies by Flood
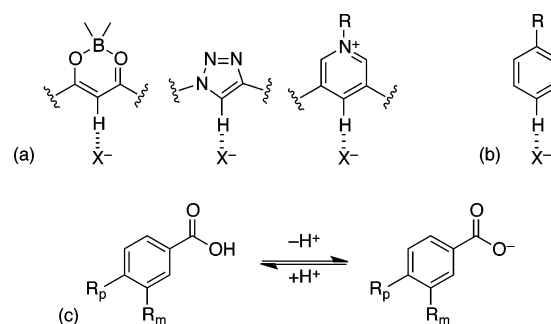

Figure 1. (a) Prototypical examples of polarized, strong CH donors. (b) Preferred benzene hydrogen bond geometries. (c) Equilibrium of benzoic acids for derivation of Hammett parameters.

et al. have sought to dissect the strength of an arene CH vs an alkyl CH.[15] A similar structure was used by Garcia Mancheño and co-workers to examine the influence of structure and electronics on catalysis;[12,13] however, neither of these investigations measured the direct effects of substituents or anions on the CH donor energy or the CH component of the total Gibbs free energy of association for these HBs. The lack of

studies on these aspects of CH HBs has led to some confusion on the characteristics, i.e., strength and selectivity, compared to traditional HB donors.

Conversely, the related interactions between anions and electron-deficient aromatic rings have been the subject of extensive computational and experimental studies that have resulted in the complete dissection of the energetic components and substituent effects.[16,17] It has also been recognized that an anion can interact with the face of an arene via anion−π or weak−σ interactions, leading to differentiation in both substituent and anion effects.[18−20] Computational studies indicate this type of dual anion and substituent dependence is important in CH HBs as well, although this has not been reduced to practice experimentally.[21] As a standard and classical physical organic tool, the use of linear free energy relationships (LFERs), particularly the Hammett equation, for probing dynamic interactions is increasingly popular.[22]

Hay et al. performed an initial study to quantify the binding energy of benzene CH HBs, wherein they described both quite strong HBs to anions in the gas phase and a linear dependence of the binding energy on substituent electron-withdrawing ability, as measured by different substituent effects.[23,24] The substituent effects in their model (Figure 1b) could be described by a Hammett σ_m or electrostatic potential (ESP).[24] The use of a Hammett σ_m parameter to describe an interaction at the *para* position is typically assumed to indicate a mostly electrostatic interaction, due to the lack of conjugation at the *meta* position in the prototypical Hammett reaction, namely, the ionization of benzoic acid (Figure 1c).[25]

The assumption of electrostatic dominance is supported by the additional correlation with ESP. A recent analysis by Scheiner et al.[21] of HBs to trifluoromethane revealed subtle energetic parameters. As included in the definition of a hydrogen bond, there exists a bond critical point between the H and X− (anion), as well as a shift in the vibrational frequency of the CH stretch.[26] These effects are driven by the partial covalency of the HB and can be accentuated by examining the changes across a series of anions.

In the course of designing selective, fluorescent anion receptors, our group recently introduced the benzene CH HB donor into our existing bisarylethynyl urea scaffold to produce **1a** (Figure 2a).[27] In this report we have sought to better understand the parameters for controlling aryl CH HB acidity with anions by substitution *para* to the CH donor, **1b−g**. The modularity of our scaffold allows us the unique chance to study a single CH···X− HB by easily accessible solution techniques: ^{1}H NMR and UV−vis spectroscopic titrations with multiple

anions (Cl−, Br−, I−, and NO$_3^-$). Association constants, K_a, are reported for seven receptors (**1a−g**) in water-saturated CHCl$_3$. Combined solution experiments, crystallography, and computations provide new insight into the preferred CH binding geometry and electronic control. Linear free energy relationships using Hammett parameters and ESP reveal ρ dependence on the anion being titrated. Multivariate analysis with Swain− Lupton field (F) and resonance (R) parameters provides a deeper understanding of the percent resonance contribution to aryl CH acidity.[28,29] Our combined experimental and computational approach for understanding CH HBs provides renewed support for the role of resonance in CH HBs. In addition, consideration of the anion in a supramolecular structure activity relationship identifies a new avenue for understanding and predicting anion binding selectivity.

RESULTS AND DISCUSSION

Synthesis and Characterization. The substituted receptors used for this study are part of the bis(2-anilino-ethynyl)arene family of conjugated, fluorescent receptors we have reported previously.[30−36] In this case, pendent methoxy substituted phenylureas act as additional HB donors to direct the anion binding into a single site, as illustrated in Figure 2b.[19,32,35] The synthesis of **1a** has been previously reported and forms the parent scaffold for our study of substituent effects.[27] These receptors are highly modular and easily broken into three key units for stepwise synthesis—a core arene, an alkynyl aniline, and an isocyanate.[36] For the current investigation, the core arene can be any 3,5-dibromo- or 3,5-diiodobenzene suitable for Sonogashira cross-coupling possessing either an electron-withdrawing or electron-donating substituent in the 1-position. The *t*-Bu group on the alkynyl aniline was used to provide solubility in noncompetitive organic solvents (i.e., CHCl$_3$). The 4-methoxy unit was chosen for the pendent phenylurea due to its simpler monomeric speciation in solution and to modulate the strength of the competing urea HBs. Such electron-rich ureas provide less competition with the CH···X− HB and have proven to be less prone toward self-aggregation.

Dianilines **2a−g** were synthesized by Sonogashira cross-coupling of 2-ethynyl-4-*tert*-butylaniline (desilylated **3**) with the corresponding dihaloarenes **4a−g** (Scheme 1). Reaction of the resulting dianilines with 4-methoxyphenyl isocyanate afforded the bisureas **1a−g**. In most cases, the bisurea could be purified by trituration with EtOH to provide analytically pure samples. Receptors **1a−g** were characterized by ^{1}H and ^{13}C NMR spectroscopy and high-resolution mass spectrometry. Complete synthetic procedures can be found in the Supporting Information (SI). The pendent ureas on our receptors are necessary to boost the overall binding energy high enough to observe in solution by ^{1}H NMR and UV−vis spectroscopy.[37] Previous efforts to study substituent effects in noncovalent interactions have been complicated by substituents altering peripheral HBs.[16,38] Gratifyingly, the ^{1}H NMR spectra of these receptors in DMSO-d_6 show a small shift in the urea protons (H$_h$ and H$_g$, Figure 3), suggesting substitution is far enough away to minimize, but not completely mitigate, the substituent effects on the ureas while still modulating the core CH HB donor acidity.[39] The closest aromatic proton to the central ring, H$_d$, shifts <0.01 ppm between the −NO$_2$ (**1b**) and −NMe$_2$ (**1g**) substituted receptors. The central ring protons, however, show a strong substitution dependence, with H$_b$ ranging from 7.0 (**1f**) to 8.5 ppm (**1b**). The isolation of substituent effects on the $\Delta\delta$ to just the central ring is necessary to measure only the
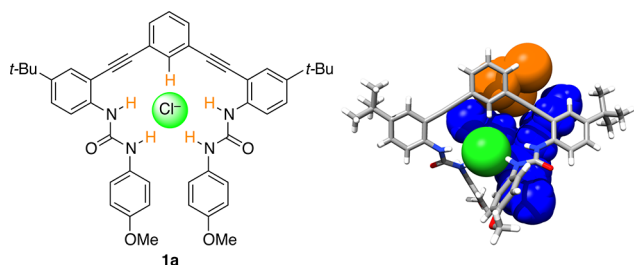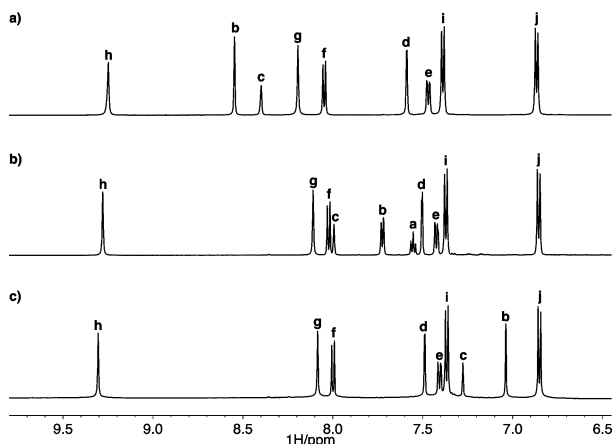

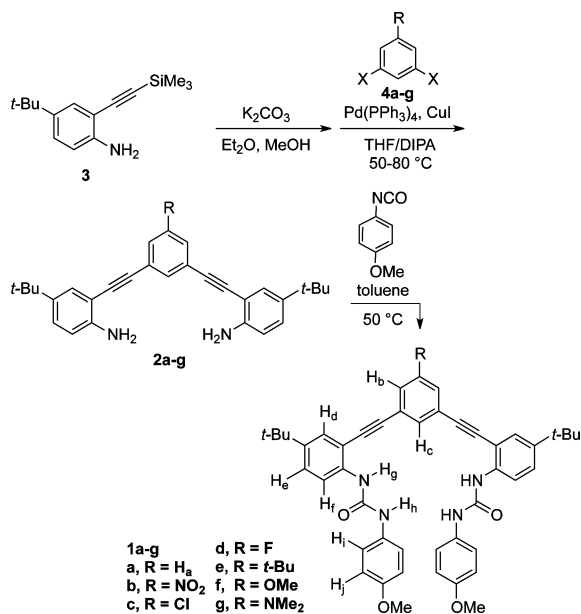**Figure 2.** (a, left) Urea anion receptor **1a** shown in optimal binding geometry for Cl−. (b, right) X-ray crystal structure of **1a**⊂Cl− with solvent (CHCl$_3$, orange) and counterion (TBA+, blue) included as space-filling models. CCDC no. 929532.

Scheme 1. Synthesis of Bisarylethynyl Urea Receptors 1a−g

Figure 3. Stacked NMR spectra of (a) **1b**, (b) **1a**, and (c) **1g** in DMSO-d_6. Proton assignments refer to Scheme 1.

effects on the CH···X$^-$ interactions without complicating secondary effects. ^{1}H NMR chemical shifts are subject to conformational changes and are insufficient evidence alone; however, calculations of Mulliken charge and ESP also support a small influence on the urea HB donors.

The solid-state structure determined by single-crystal X-ray diffraction is consistent with our structural characterization and solution behavior as studied previously by NMR, including 2D ^{1}H−^{13}C HSQC.[27] A single crystal of **1a·Cl$^-$** was obtained by slow evaporation of CHCl$_3$ containing a 2-fold excess of TBACl. The previously reported structure of **1a·Cl$^-$** has a short, linear C(H)···Cl contact of 3.579(3) Å and 169° (∠C−H···Cl). The asymmetric unit is a 1:1 receptor:anion complex with a cocrystallized tetrabutylammonium (TBA) cation and solvent molecule (Figure 2b). The presence of a 1:1 complex is encouraging for binding in solution and is consistent with other examples of this scaffold.[32,34,36,40,41] The packing of this structure is dominated by ion pairing between Cl$^-$ and TBA$^+$, with dispersion interactions playing a secondary role. The lack of interhost HBs or π−π stacking interactions also suggested a decreased likelihood of aggregation in solution.

The structure of bisurea **1b** was determined from a single crystal grown by vapor diffusion of *n*-hexane into CH$_3$CN. Host **1b**, in the absence of a guest anion, forms long columnar stacks with urea HBs and π−π interactions stitching the layers together (Figure 4a). Columns are held together by dispersion
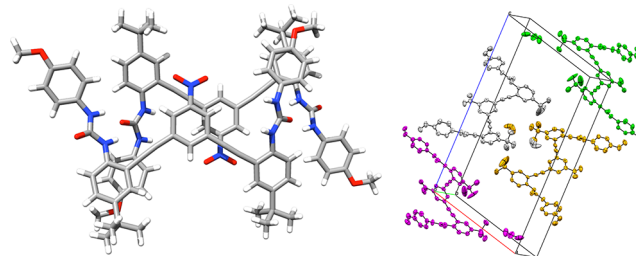
Figure 4. (a, left) X-ray crystal structure of **1b**, showing hydrogen-bonded stacks. (b, right) Packing of **1b**.

forces between alkyl groups (*t*-Bu and Me) and arrange into a herringbone pattern (Figure 4b). The propensity for **1b** to form hydrogen-bonded aggregates is embodied by poor solubility and aggregation at high concentrations in solution limiting the maximum concentration during ^{1}H NMR titration experiments.

NMR Titrations. ^{1}H NMR titrations were performed to study the substituent effects in solution on the anion binding conformation and CH chemical shift. The magnitude and direction of the change in chemical shift are additional parameters set out in the HB definition for the presence and strength of a HB (instead of an alternative attractive force, such as dispersion).[26] Consistent with previous studies on anion−π interactions,[17] water-saturated CHCl$_3$ was used as the solvent, and anions were added as their TBA salts. Titrations were performed keeping the host concentrations constant (starting at 0.5−1.5 mM) during an experiment and titrating in a solution of concentrated anion in a solution of the host. Urea proton chemical shift changes between hosts are similar to the small changes observed in DMSO (see SI).

A representative titration is shown in Figure 5. This example of unsubstituted receptor **1a** follows the trends for all of the receptors. The alkyl protons (*t*-Bu and OMe) remain unchanged throughout the course of anion addition (see the SI for complete titration data). The urea proton (H$_h$) and the
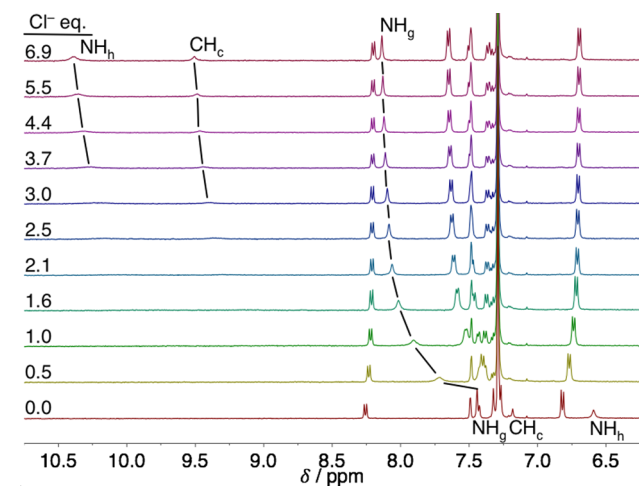

Figure 5. Representative stacked plot for a Cl$^-$ titration with host **1a** in water-saturated CHCl$_3$ using a TBA salt.

Table 1. Complete Association Constants and Binding Energy for Receptors 1a–g at 298 K

host (R)	Cl⁻ [a]		Br⁻ [a]		I⁻ [b]		NO₃⁻ [a]	
	K_a (M⁻¹)	ΔG (kcal mol⁻¹)	K_a (M⁻¹)	ΔG (kcal mol⁻¹)	K_a (M⁻¹)	ΔG (kcal mol⁻¹)	K_a (M⁻¹)	ΔG (kcal mol⁻¹)
1a (H)	6750 ± 600[c]	−5.22 ± 0.05	1630 ± 120[c]	−4.38 ± 0.04	150 ± 10[c]	−2.97 ± 0.03	3310 ± 170	−4.80 ± 0.03
1b (NO₂)	24600 ± 3500	−5.99 ± 0.09	5830 ± 510	−5.13 ± 0.05	580 ± 30	−3.76 ± 0.03	10600 ± 800	−5.49 ± 0.04
1c (Cl)	7900 ± 1300	−5.32 ± 0.09	2680 ± 230	−4.67 ± 0.05	290 ± 10	−3.36 ± 0.03	5520 ± 640	−5.10 ± 0.07
1d (F)	6760 ± 620	−5.22 ± 0.05	2340 ± 180	−4.59 ± 0.05	240 ± 10	−3.25 ± 0.03	4810 ± 320	−5.02 ± 0.04
1e (tBu)	4560 ± 720	−4.99 ± 0.09	1370 ± 100	−4.28 ± 0.03	150 ± 10	−2.98 ± 0.04	2700 ± 420	−4.68 ± 0.09
1f (OMe)	4730 ± 240	−5.01 ± 0.03	1000 ± 70	−4.09 ± 0.04	170 ± 10	−3.02 ± 0.03	3060 ± 360	−4.75 ± 0.07
1g (NMe₂)	2660 ± 320	−4.67 ± 0.07	800 ± 40	−3.96 ± 0.03	100 ± 10	−2.74 ± 0.07	1720 ± 160	−4.41 ± 0.05

[a]Determined using UV−vis titrations in H₂O-saturated CHCl₃; error is the standard deviation (SD) of at least three titrations. [b]Determined using ¹H NMR titrations in H₂O-saturated CDCl₃; error is the SD of at least two titrations. The minimum error is assumed to be 5% in cases where the SD is <5%. [c]Previously reported (ref 27).

CH proton (H_c) are unresolved during most of the titration, which may be due to the large shifts ($\Delta\delta = 4.0$ and 2.5 ppm) between the free host and the saturated host:Cl⁻ complex. Although the broadening prevents fitting these peaks for an association constant (K_a), the large, downfield shifts indicate strong HBs with H_h and H_c. Fortunately, the other aromatic and urea protons remain well resolved throughout the titration, except for brief periods of overlap for some peaks. Urea H_g shifts downfield with anion binding, while the aromatic protons remain stationary or move upfield slightly. The decreased broadening and smaller $\Delta\delta$ for H_g, observed for the halides with all hosts, is evidence for an overall weaker HB to this urea proton.

The chemical shift change of urea NH_g was fit using nonlinear regression analysis in MatLab to a 1:1 host:guest model.[42] This model was selected based on the crystallographic evidence for 1:1 binding and quality of fit compared to higher order models. The trend for association constants follows the general electron-withdrawing ability of the substituents and the expected Hoffmeister bias (Cl⁻ > NO₃⁻ > Br⁻ ≫ I⁻).[43,44] The large association constants measured for Cl⁻ (>10⁵ M⁻¹ in some cases) indicates NMR spectroscopy is not the ideal technique for determining high quality association constants. Strong EWG hosts (**1b**) with Cl⁻ are at the upper limit for measuring K_as by NMR titrations and the fit is based on a single proton shift. We can make a qualitative analysis of the bound geometry and trends, but the further quantitative analysis is based on UV−vis titrations (Table 1).

The ¹H NMR spectra of the bound receptors are remarkably similar considering the variety of substituents used (Figure 6). As with the free receptors, the largest variation of $\Delta\delta$ is seen for two equivalent phenyl H_b resonances. The final δ for the urea protons, H_g and H_h, changes <0.1 ppm for all of the receptors. The only peak that shows a large change is the aromatic core CH_c, where there is a difference of 1.2 ppm between **1b·Cl⁻** and **1g·Cl⁻**. Subtracting the difference before anion binding (Figure 3) leaves $\Delta\delta = 0.2$ ppm due to a change in the HB strength. Also of note, the final position follows the trend of EWG strength. A similar trend is observed for Br⁻ and I⁻ binding, albeit with smaller $\Delta\delta$ for H_h and H_c. The chemical shift of the internal urea proton H_g changes minimally when bound to Br⁻, I⁻, or Cl⁻, consistent with it being mostly peripheral to halide binding.

In addition to the halides, titrations were also performed with nitrate to consider shape as a variable in the binding studies (Figure 7, top). While the halides are spherical and have very small preference for HB arrangements, nitrate is trigonal planar and prefers a bifurcated, O···(C)H···O structure (Figure 7,
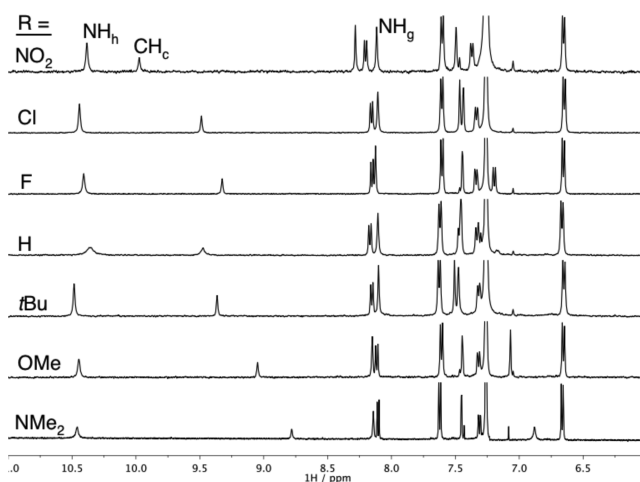

Figure 6. ¹H NMR spectra (CDCl₃) of receptors **1a–g** near the saturation point with Cl⁻. The peak showing the largest shift between 8.8 and 10.0 ppm is that of aryl proton H_c. Peak assignment refers to Scheme 1.

bottom).[21] In this case, the hydrogen-bonding protons NH_h and CH_c shifted less than observed with the halides, and urea NH_g ends up slightly farther downfield. Considering the likely geometries for nitrate binding, the relative chemical shifts point to a geometry where two oxygens are bound by NH_g and bifurcated by CH_c; the third oxygen only weakly interacts with NH_h. Modeling of the nitrate complex in Figure 7 supports this hypothesis, with two local minima, from divergent starting structures, found with nitrate parallel to the CH bond. With confirmation that the anions were bound in a similar manner by all of the receptors in solution, we sought to obtain quantitative association constants by performing UV−vis titrations.

UV−Vis Titrations and Association Constants. The rigid, conjugated arylethynyl backbone used in these receptors has the added benefit of providing a convenient absorbance for performing UV−vis titrations.[36] Although they do not provide as much structural information as NMR, UV−vis titrations are more accurate in determining K_as for our system because the required receptor concentrations are lowered (limiting aggregation), and problems with disappearing or overlapping peaks present in ¹H NMR studies cease. The conditions for UV−vis titrations were chosen to most closely match the ¹H NMR binding experiments: water-saturated CHCl₃ was used as solvent and anions as their TBA salts were monitored at 298 K. Association constants were determined using the HYPERquad 2006 package to fit the complete spectral window with
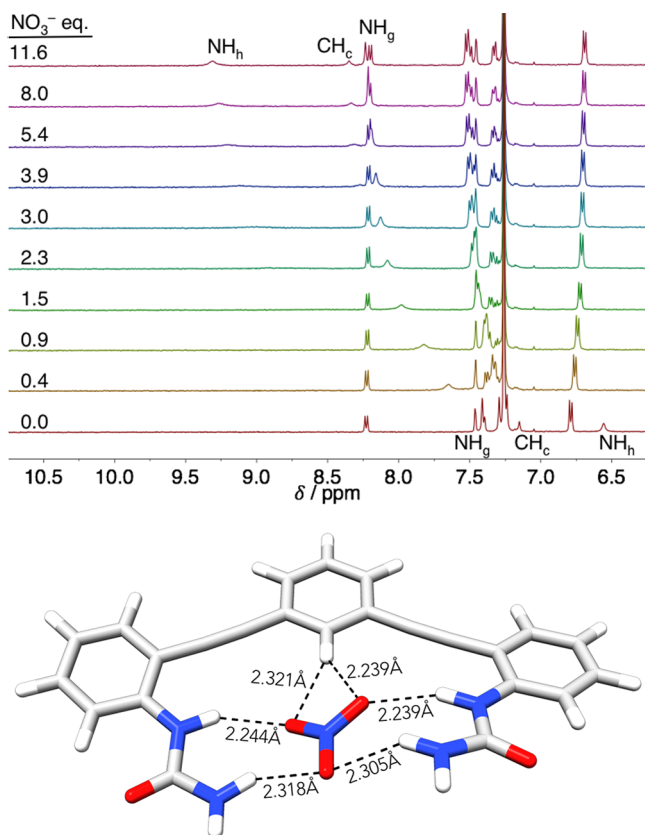
Figure 7. (Top) Stacked plots showing the NO_3^- titration of **1a**. (Bottom) Local minima of truncated **5a·NO_3^-**, with distances showing the preference of NO_3^- for maximized urea contacts and a bifurcated CH hydrogen bond. B3LYP/6-31g(d).

nonlinear regression.[45] Consistent with the ^{1}H NMR experiments, all titrations were fit to a 1:1 binding isotherm. Job's plot analysis also confirms the best fit model for selected host and anion combinations (see SI).

Table 1 contains the compiled association constants for receptors **1a–g** with Cl$^-$, Br$^-$, I$^-$, and NO_3^-. The selectivity of these receptors follows this preference, with the trend of Cl$^-$ > NO_3^- > Br$^-$ ≫ I$^-$ holding for all hosts. The chloride association constants are typically 3-fold higher than the bromide K_as. Interestingly, nitrate is not able to outcompete Cl$^-$ despite nitrate's ability to maximize NH HBs. The extremely low association for iodide prevented the accurate determination of binding constant by UV–vis spectrophotometry and necessitated the use of ^{1}H NMR binding data for further analysis.

The range of association constants for Cl$^-$ alone spans an order of magnitude, with just altering a single arene substituent. Consistent with the changes in chemical shift, the association constants for a given anion can be ranked according to the relative electron-withdrawing ability of the substituent. Surprisingly, fluorine is an outlier for the trend in eletronegativity of the substituent. Fluorine typically acts as an electron-withdrawing group for electrostatic interactions, except when resonance is a contributor. Fluorine acts as both a strong electron-withdrawing group due to induction and an electron-donating group by resonance with one of its lone pairs. Other groups in this table (OMe, NMe$_2$, Cl) share this dual function and are important for differentiating between induction and resonance effects. The association constants

have also been converted to ΔG (kcal mol^{-1}) for comparison to other supramolecular receptors. The total binding energy can be tuned by substituent effects by 1.02–1.32 kcal mol^{-1} depending on the anion being titrated; i.e., Cl$^-$ is bound more strongly than I$^-$ by 1.92–2.23 kcal mol^{-1} throughout this class of receptors.

Computations. Prior computations on model structures of chloride and nitrate with benzene showed CH HB strength (ΔH) follows linearly with the Hammett σ parameters and ESP.[23,24] We have expanded upon these prior computations by calculating the ESP surfaces for the model systems **5** and **6** (Figure 8) to measure electrostatic contributions in the bisurea
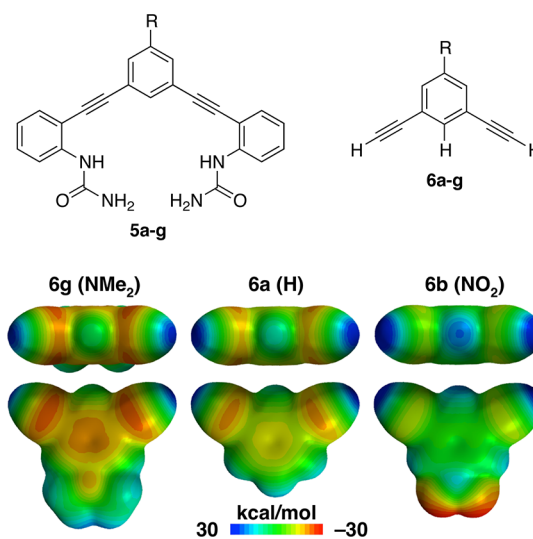

Figure 8. (Top) Structures of the truncated model compounds **5** and **6** used for computational studies. (Bottom) MESP maps showing effects of substituent on ESP at a 0.002 Å isoelectric surface, calculated using B3LYP/6-31+g(d) in Spartan '10.

receptors. The primary metric from these calculations is the ESP of **6a–g** (Table 2) at the point where the C–H axis

Table 2. Computational and Empirical Values for LFER Analysis

host (R)	ESP	σ_m[25]	σ_p[25]	F[29]	R[29]
1b (NO$_2$)	28.9	0.71	0.78	1.00	1.00
1c (Cl)	22.1	0.37	0.23	0.72	−0.24
1d (F)	21.4	0.34	0.06	0.74	−0.39
1a (H)	17.9	0.00	0.00	0.00	0.00
1e (tBu)	16.3	−0.10	−0.20	−0.11	−0.29
1f (OMe)	16.3	0.12	−0.27	0.54	−1.68
1g (NMe$_2$)	12.0	−0.15	−0.83	0.69	−3.81

[a]ESP (kcal mol^{-1}) at the point where the CH bond intersects a 0.002 Å isoelectric surface, calculated using B3LYP/6-31+g(d) in Spartan '10.

intercepts the 0.002 Å isoelectronic surface. The ESP at this point trends with the electron-withdrawing ability of the substituents. Hammett plots of the ESP (**6a–g**, Table 2 and Figure S52) and σ parameters favor σ_p over σ_m, with R^2 = 0.97 and 0.88, respectively. This is a first indication that interactions with the CH are dependent on both field/inductive and resonance contributions of the substituents.

The bisurea model system **5a–g** is also useful to measure whether substitution at the central arene affects the urea group.

A change in the Mulliken charge on the hydrogen-bond-donating carbon and nitrogens is representative of the effects at each of these positions. The Hammett plot of Mulliken charge at the hydrogen-bond-donating carbon in **5** is linear with σ_p, R^2 = 0.90 and $\rho = -0.10 \pm 0.02$. Mulliken charges on the urea nitrogens produce Hammett plots for σ_p and σ_m with very poor fits, $R^2 \leq 0.70$ and $\rho \approx 0.007 \pm 0.002$ (Table S43). Substitution on the central arene has very weak through-bond effect on the ureas in this system. The through-space effect is better estimated by the ESP near the urea hydrogens. In this case, Hammett plots reveal the change at the urea is <50% of the change at the CH donor. This model, however, does not account for the electron-donating pendent phenyls in the full receptor, **1a–g**, which would further diminish the influence of the ureas.

Linear Free Energy Relationships. Linear free energy plots of the ESP and association constants are one way of comparing computational and experimental results, bridging the gap between gas phase and solution.[46] Non-normalized plots in kcal mol^{-1} are linear, with $R^2 > 0.95$ for all four anions (Figure 9). A break in the trend of the fitted slopes appears
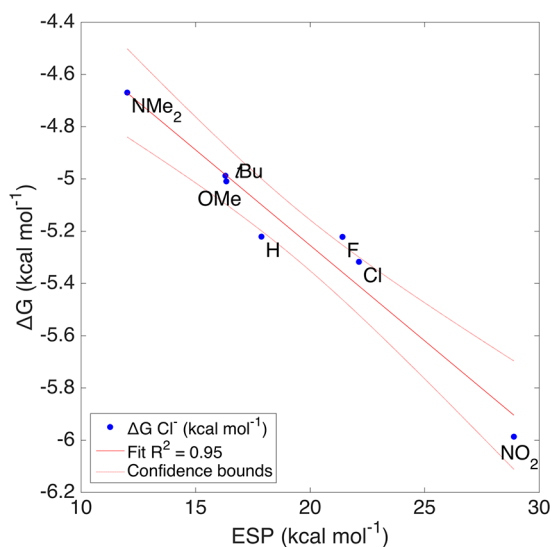

Figure 9. Linear free energy relationship of the solution Gibbs free energy (ΔG) of binding for Cl$^-$ with the ESP at the CH bond. Intercept predicts a hypothetical system where electrostatic potential is zero.

between the harder anions (Cl$^-$ and Br$^-$) and soft anions (I$^-$ and NO$_3^-$). The hardness of anions has been used to explain the selectivity of Cl$^-$ transport in micelles, although alternative explanations have not been conclusively ruled out.[47]

Another interesting implication falls out of the intercept in these plots. When the ESP is reduced to zero at the intercept, the remaining binding energy is due to the non-CH interactions. This is based on an assumption that the electrostatics model completely or mostly describes the CH···X interaction. As would be expected the intercept follows the same trend in energies (kcal mol^{-1}), Cl$^-$ = -3.79, NO$_3^-$ = -3.67, Br$^-$ = -3.06, I$^-$ = -1.98. The remaining "CH hydrogen bond energies" after subtracting the intercept from the solution ΔG for **1b** are -2.20, -1.82, -2.07, and -1.78 kcal mol^{-1} for each anion, respectively. Previous studies with this system compared **1a** to a pyridine receptor and estimated the CH HB energy at -1.33 kcal mol^{-1} to Cl$^-$.[27] In this case, the estimated

energy for **1a** with Cl$^-$ is quite close, at -1.43 kcal mol^{-1}. Nitrate is a clear outlier in this series based on its preference for a bifurcated HB. The CH HB is less important for nitrate; however, using this model 47% of the total binding energy for iodide originates from the CH HB solely.

Since the substitution is only on the central arene and appears to only affect the C–H$_c$ proton, we hypothesized that trends in our association constants should, also, be well-described by the σ parameter for substituents. The Hammett plots for Cl$^-$, Br$^-$, I$^-$, and NO$_3^-$ were prepared for both σ_m and σ_p constants. Figure 10 compares the fit for σ_p with K_a (Cl$^-$)
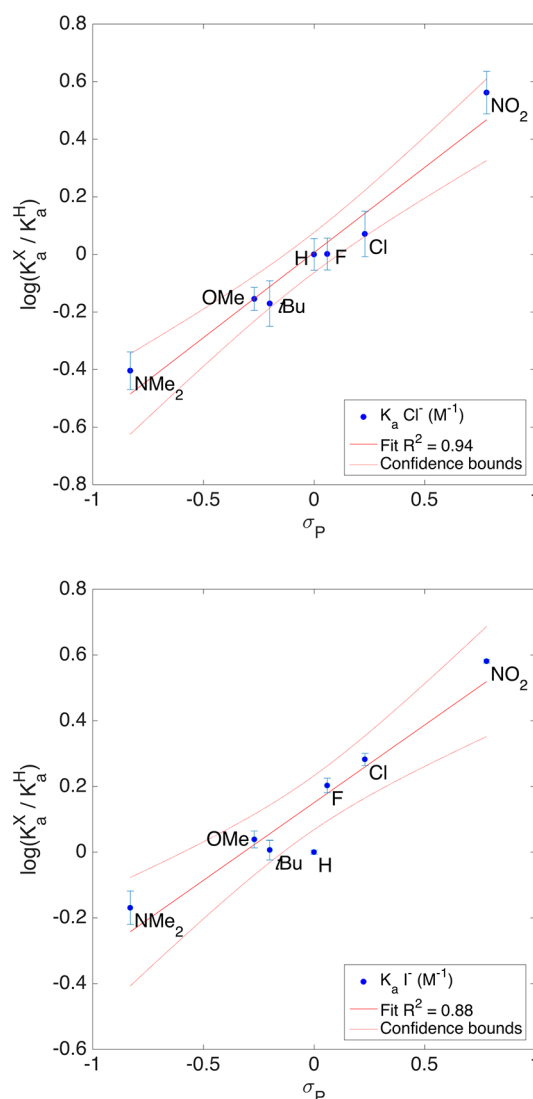

Figure 10. Hammett plots of K_a (Cl$^-$) (top) and K_a (I$^-$) (bottom) with σ_p (Table 2). Goodness of fit (R^2) indicates Cl$^-$ is well described by σ_p, while I$^-$ is less well-described.

and K_a (I$^-$). Association constants and substituent parameters were fit using the Hammett equation (eqs 1 and 2) in MatLab. The intercept acts as another measure for the quality of fit. In this case, the large intercept for I$^-$, a poor fit for σ_p, places **1a** outside of the confidence bounds (Figure 10 bottom). Table 3 contains the complete results for fitting all four anions to σ_p and σ_m.[48]

$$\log(K_R/K_H) = \rho\sigma_p + i \tag{1}$$

$$(K_a\ Cl^-)\ \log(K_R/K_H) = 0.59(\pm0.06)\sigma_p + 0.01(\pm0.03),$$

$$N = 7, \quad R^2 = 0.95, \quad R_{adj}^2 = 0.94,$$

$$RMSE = 0.07, \quad F = 100 \tag{2}$$

Table 3. Coefficients and Fitting Statistics for Hammett Plots for Each Anion Studied

K_a (X^-)	ρ	I^a	N^b	$R^{2\ c}$	F^d
Cl^- (σ_p)	0.59($\pm$0.06)	0.01($\pm$0.03)	7	0.95	100
Br^- (σ_p)	0.57($\pm$0.07)	0.07($\pm$0.03)	7	0.93	68
I^- (σ_p)	0.47($\pm$0.07)	0.15($\pm$0.03)	7	0.90	46
NO_3^- (σ_p)	0.50($\pm$0.05)	0.09($\pm$0.02)	7	0.95	98
Cl^- (σ_m)	0.89($\pm$0.18)	$-$0.18($\pm$0.06)	7	0.83	25
Br^- (σ_m)	0.87($\pm$0.16)	$-$0.11($\pm$0.06)	7	0.85	28
I^- (σ_m)	0.78($\pm$0.08)	$-$0.01($\pm$0.03)	7	0.95	102
NO_3^- (σ_m)	0.80($\pm$0.09)	$-$0.08($\pm$0.03)	7	0.94	83

^{a}Intercept obtained from the linear fit. ^{b}Number of points used for fitting. ^{c}Coefficient of determination for quality of fit determination. ^{d}F-value for comparison of models.

The ρ values for all combinations of σ and anion are <1, an average of 0.54 for σ_p and 0.85 for σ_m. Reactions with ρ values >1 are considered more sensitive than benzoic acid and ρ values <1 are less sensitive to ionization by substituent effects. If CH··· X^- is a HB and incorporates some covalent character, then it follows that there is a small proton transfer event contributing to the binding energy.[26] The method of fitting anion association to a Hammett σ_p is also applicable to other CH HB anion receptors. For instance, it is interesting to note, at least preliminarily, that a Hammett plot of Cl^- association to a CH hydrogen-bond-donating rotaxane host has $\rho = 0.53$.[49] The similarity of this relationship to a very different host in a different solvent is encouraging, and suggests this understanding is extendable to other such systems.

The question remains, has the influence of the urea HB donors been sufficiently accounted for? The ρ for Hammett plots of Mulliken charge and ESP at the ureas is consistently <0.06. The change in association constant due to the ureas is estimated to be <10% based on this and is insufficient to explain the effects on the binding event.

The small ρ value is consistent with the CH bond being much less acidic than benzoic acid. Also consistent with a traditional hydrogen bond definition, the σ_p parameter has a better fit for Cl^- than σ_m (R^2 (σ_p) = 0.95 vs (σ_m) = 0.83). σ_p is often thought to represent a greater resonance contribution; however, two points conflict with this observation: (1) DFT calculations favored σ_m for Cl^-,[24] and (2) the results for I^- do not match Cl^-, where Hammett plots for I^- are a better fit using σ_m. Further confounding the issue, NO_3^- is well described by both σ_p and σ_m.

The unusual results for NO_3^- can be described by the geometry and altered binding mode in this case. The oxoanion is trigonal planar and can maximize contacts to the NH donors, as discussed above; however, the CH donor is still important to the overall binding energy. The CH proton still shifts downfield by nearly the same magnitude as the NH protons. The observed ρ values are the result of both inductive and resonance contributions. The degree of resonance contribution is a key difference between the σ_m and σ_p parameters.

A more accurate method for determining resonance contribution is to perform multivariable fitting with field (F)

and resonance (R) parameters, such as those derived by Swain and Lupton.[28,29] While many methods for determining field and resonance contribution have been proposed, the F and R parameters (Table 4) developed by Swain−Lupton most

Table 4. Field and Resonance Fitting Parameters

	ρ_f	ρ_r	R^2	$\%R^a$
Cl^-	0.36($\pm$0.09)	0.17($\pm$0.02)	0.937	32 $\pm$ 7
Br^-	0.37($\pm$0.03)	0.15($\pm$0.01)	0.995	30 $\pm$ 6
I^-	0.40($\pm$0.05)	0.14($\pm$0.01)	0.977	25 $\pm$ 3
NO_3^-	0.37($\pm$0.02)	0.14($\pm$0.01)	0.996	28 $\pm$ 1

^{a}Calculated from eq 4 for percent resonance.

closely match Hammett's σ parameters in their derivation (eq 3). MatLab is capable of handling large, multivariable linear regressions and can easily handle fitting values for F and R from the data presented above. The method was applied to the experimental K_a values and the results for Cl^- are plotted in Figure 11. A figure of merit for simultaneous F and R fitting is the percent resonance contribution, $\%R$ (eq 4).

$$\log(K_X/K_H) = \rho fF + \rho rR + i \tag{3}$$
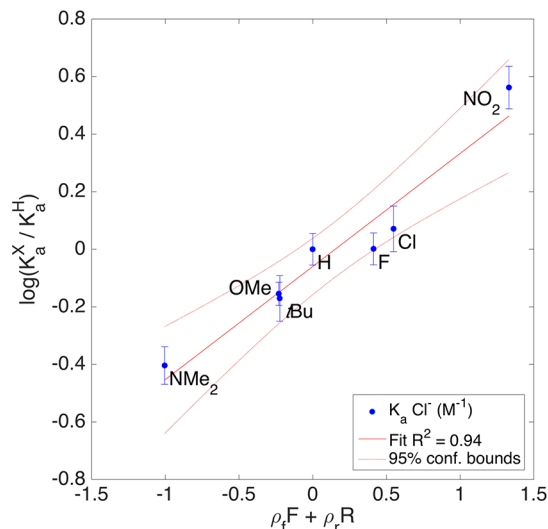
$$\%R = \rho r/(\rho f + \rho r) \times 100 \tag{4}$$

Figure 11. LFER plot of K_a (Cl^-) and $\rho_f F + \rho_r R$ to determine resonance contribution from Swain−Lupton field and resonance parameters.

This reports the resonance contribution observed in the reaction and is the percent of R from the combined ρf and ρr coefficients. Of note, the resonance contribution for Cl^- and Br^- is higher, but the values drop off for I^- and NO_3^-. The error values in $\%R$ exceed 10% in most cases, which is due to the small sample size to variable ratios. As a result of the increasing number of variables, the difference in the $\%R$ contribution among the various anions studied is well below the 95% confidence interval by t test. A similar trend, however, in anion effects was observed by Scheiner et al. using computation to study anion binding to trifluoromethane.[21] By their computations, the overall binding energy and charge transfer from the anion were correlated, consistent with the effect of resonance contribution we have observed. As in the extreme

HB example, increased charge on the carbon can be dissipated by resonance and contribute additional HB energy beyond inductive effects alone.

CONCLUSIONS

The resonance contribution of a substituent clearly plays a role in dictating hydrogen bond strength, even for CH donors. We have observed a weak dependence of σ_p and σ_m contribution on the anion being bound. Hammett parameters remain a powerful tool for predicting changes in CH HB strength. It is important to also consider the HB acceptor, not only its charge but also size, shape, and polarizability. The change in resonance contributions as a result of substituent effects as calculated by Swain−Lupton parameters is too small to differentiate between the anions studied, suggesting that emerging hypotheses offering hard/soft acid/base theory as a model for understanding anion binding specificity are overly simplistic. Anion effects on resonance contribution are also supported by calculations of the charge transfer energy and bond stretching in model CH⋯X^- systems.

Computationally determined binding energies are a valuable tool for understanding solution binding events, especially in the case of weak interactions. Remarkably, venerable empirical substituent constants such as σ, F, and R can also effectively describe substituent effects in CH HBs, which are increasingly appreciated as rivals to more well-studied, highly polar HB donors (e.g., N−H, O−H). We have found through experimental results that the strength of a single CH HB is tunable across a range of $1.02-1.23$ kcal mol^{-1} by modifying substituents on the receptor and that these interactions vary up to 0.42 kcal mol^{-1} by changing the anion accepting the CH HBs. Although these values are small, they represent a 10-fold and 3-fold change in anion binding, respectively, and hint at the nature of anion binding selectivity in such receptors. Considering multivalent effects in the largest hydrogen-bond-donating receptors that bring to bear many such interactions in targeting a single anion, the combined effect can be used to dramatically alter the binding event in selectivity and strength. While hard/soft acid/base theory remains a useful tool in understanding coordination chemistry, the present studies add to the evidence that this theory is too simplistic to describe accurately the nature of selectivity in anion binding using hydrogen-bonding receptors; ESPs and other empirical substituent constants appear to provide a more robust understanding.

Aryl CH HBs have seen increasing study in numerous fields, including anion transport, organocatalysis, molecular/ion recognition, and biological ligand/receptor binding. New methods for understanding and controlling the strength and selectivity of these interactions are vital for continued progress in these fields. For instance, ligand and/or drug binding to proteins can be improved by studying and optimizing important CH hydrogen-bonding interactions, and enhancing such interactions in organocatalysis and receptor design may enable improved stereo- and regioselectivity. Although the CH donor cannot be easily categorized as hard or soft, we have made the more important discovery that the possibility exists to influence the preference of this interaction for different anions. A concerted effort to maximize both the resonance withdrawing ability of substituents and the number of CH HB donors should lead to an increased affinity for hard anions. Conversely, the same should be possible by maximizing the inductive substituents to bind soft anions. The results from this study provide important insights to aid chemists and biologists in accomplishing such CH HB optimization.

ASSOCIATED CONTENT

Ⓢ Supporting Information

The Supporting Information is available free of charge on the ACS Publications website at DOI: 10.1021/jacs.5b08767.

> Complete synthesis and characterization for all compounds, and representative titrations for all anions (PDF)
> X-ray data for **1b** (CIF)
> Atomic coordinates and absolute energies for all computed structures (PDF)

AUTHOR INFORMATION

Corresponding Authors
*haley@uoregon.edu
*dwj@uoregon.edu

Notes
The authors declare the following competing financial interest(s): NIH grant R01-GM087398 funded early-stage intellectual property that was licensed by SupraSensor Technologies, a company co-founded by the principal investigators.

REFERENCES

(1) Cai, J.; Sessler, J. L. *Chem. Soc. Rev.* **2014**, *43*, 6198−6213.
(2) Steiner, T.; Desiraju, G. R. *The Weak Hydrogen Bond in Structural Chemistry and Biology*; Oxford University Press: Oxford, 1999.
(3) Lee, S.; Flood, A. H. In *Topics in Heterocyclic Chemistry*; Gale, P. A., Dehaen, W., Eds.; Springer: Berlin, 2012; Vol. *28*, pp 85−107.
(4) Hua, Y.; Flood, A. H. *Chem. Soc. Rev.* **2010**, *39*, 1262−1271.
(5) McDonald, K. P.; Hua, Y.; Flood, A. H. In *Topics in Heterocyclic Chemistry*; Gale, P. A., Dehaen, W., Eds.; Springer: Berlin, 2010; Vol. *24*, pp 341−366.
(6) Johnston, R. C.; Cheong, P. H.-Y. *Org. Biomol. Chem.* **2013**, *11*, 5057−5064.
(7) Desiraju, G. R. *Acc. Chem. Res.* **1996**, *29*, 441−449.
(8) Horowitz, S.; Trievel, R. C. *J. Biol. Chem.* **2012**, *287*, 41576−41582.
(9) Lee, S.; Flood, A. H. *J. Phys. Org. Chem.* **2013**, *26*, 79−86.
(10) Hua, Y.; Liu, Y.; Chen, C.-H.; Flood, A. H. *J. Am. Chem. Soc.* **2013**, *135*, 14401−14412.
(11) Maeda, H.; Kitaguchi, K.; Haketa, Y. *Chem. Commun.* **2011**, *47*, 9342−9344.
(12) Beckendorf, S.; Asmus, S.; Mück Lichtenfeld, C.; García Mancheño, O. *Chem. - Eur. J.* **2013**, *19*, 1581−1585.
(13) Asmus, S.; Beckendorf, S.; Zurro, M.; Mück Lichtenfeld, C.; Fröhlich, R.; García Mancheño, O. *Chem. - Asian J.* **2014**, *9*, 2178−2186.
(14) Lee, S.; Chen, C.-H.; Flood, A. H. *Nat. Chem.* **2013**, *5*, 704−710.
(15) Hua, Y.; Ramabhadran, R. O.; Uduehi, E. O.; Karty, J. A.; Raghavachari, K.; Flood, A. H. *Chem. - Eur. J.* **2011**, *17*, 312−321.
(16) Ballester, P. *Acc. Chem. Res.* **2013**, *46*, 874−884.

(17) Adriaenssens, L.; Gil-Ramírez, G.; Frontera, A.; Quiñonero, D.; Escudero-Adán, E. C.; Ballester, P. *J. Am. Chem. Soc.* **2014**, *136*, 3208−3218.

(18) Berryman, O. B.; Hof, F.; Hynes, M. J.; Johnson, D. W. *Chem. Commun.* **2006**, 506−508.

(19) Watt, M. M.; Collins, M. S.; Johnson, D. W. *Acc. Chem. Res.* **2013**, *46*, 955−966.

(20) Wang, D.-X.; Wang, M.-X. *J. Am. Chem. Soc.* **2013**, *135*, 892−897.

(21) Nepal, B.; Scheiner, S. *Chem. - Eur. J.* **2015**, *21*, 1474−1481. Scheiner, S.; Grabowski, S. J.; Kar, T. *J. Phys. Chem. A* **2001**, *105*, 10607−10612.

(22) Hwang, J.; Li, P.; Carroll, W. R.; Smith, M. D.; Pellechia, P. J.; Shimizu, K. D. *J. Am. Chem. Soc.* **2014**, *136*, 14060−14067. Wheeler, S. E.; McNeil, A. J.; Müller, P.; Swager, T. M.; Houk, K. N. *J. Am. Chem. Soc.* **2010**, *132*, 3304−3311. Zhou, Y.; Yuan, Y.; You, L.; Anslyn, E. V. *Chem. - Eur. J.* **2015**, *21*, 8207−8213. Zhou, Y.; Ye, H.; You, L. *J. Org. Chem.* **2015**, *80*, 2627−2633.

(23) Bryantsev, V. S.; Hay, B. P. *J. Am. Chem. Soc.* **2005**, *127*, 8282−8283.

(24) Bryantsev, V. S.; Hay, B. P. *Org. Lett.* **2005**, *7*, 5031−5034.

(25) Hansch, C.; Leo, A.; Taft, R. W. *Chem. Rev.* **1991**, *91*, 165−195.

(26) Arunan, E.; Desiraju, G. R.; Klein, R. A.; Sadlej, J.; Scheiner, S.; Alkorta, I.; Clary, D. C.; Crabtree, R. H.; Dannenberg, J. J.; Hobza, P.; Kjaergaard, H. G.; Legon, A. C.; Mennucci, B.; Nesbitt, D. J. *Pure Appl. Chem.* **2011**, *83*, 1637−1641.

(27) Tresca, B. W.; Zakharov, L. N.; Carroll, C. N.; Johnson, D. W.; Haley, M. M. *Chem. Commun.* **2013**, *49*, 7240−7242.

(28) Swain, C. G.; Lupton, E. C. *J. Am. Chem. Soc.* **1968**, *90*, 4328−4337.

(29) Swain, C. G.; Unger, S. H.; Rosenquist, N. R.; Swain, M. S. *J. Am. Chem. Soc.* **1983**, *105*, 492−502.

(30) Johnson, C. A., II; Berryman, O. B.; Sather, A. C.; Zakharov, L. N.; Haley, M. M.; Johnson, D. W. *Cryst. Growth Des.* **2009**, *9*, 4247−4249.

(31) Gavette, J. V.; Mills, N. S.; Zakharov, L. N.; Johnson, C. A.; Johnson, D. W.; Haley, M. M. *Angew. Chem., Int. Ed.* **2013**, *52*, 10270−10274.

(32) Gavette, J. V.; Evoniuk, C. J.; Zakharov, L. N.; Carnes, M. E.; Haley, M. M.; Johnson, D. W. *Chem. Sci.* **2014**, *5*, 2899−2905.

(33) Watt, M. M.; Engle, J. M.; Fairley, K. C.; Robitshek, T. E.; Haley, M. M.; Johnson, D. W. *Org. Biomol. Chem.* **2015**, *13*, 4266−4270.

(34) Watt, M. M.; Zakharov, L. N.; Haley, M. M.; Johnson, D. W. *Angew. Chem., Int. Ed.* **2013**, *52*, 10275−10280.

(35) Engle, J. M.; Carroll, C. N.; Johnson, D. W.; Haley, M. M. *Chem. Sci.* **2012**, *3*, 1105−1110.

(36) Vonnegut, C. L.; Tresca, B. W.; Johnson, D. W.; Haley, M. M. *Chem. - Asian J.* **2015**, *10*, 522−535.

(37) Yoon, D.-W.; Gross, D. E.; Lynch, V. M.; Sessler, J. L.; Hay, B. P.; Lee, C.-H. *Angew. Chem., Int. Ed.* **2008**, *47*, 5038−5042.

(38) McGrath, J. M.; Pluth, M. D. *J. Org. Chem.* **2014**, *79*, 11797−11801.

(39) DMSO was chosen in this case because it is a highly competitive solvent and allows for high receptor concentration without fear of aggregation or saturation. The DMSO also acts to bind to the ureas, as indicated by their downfield shifts, decreasing the anion binding strength and making it a poor solvent for titrations. As well, the hydroscopic nature of DMSO hinders attempts to accurately control the water content between experiments.

(40) Carroll, C. N.; Berryman, O. B.; Johnson, C. A.; Zakharov, L. N.; Haley, M. M.; Johnson, D. W. *Chem. Commun.* **2009**, 2520−2522.

(41) Carroll, C. N.; Coombs, B. A.; McClintock, S. P.; Johnson, C. A., II; Berryman, O. B.; Johnson, D. W.; Haley, M. M. *Chem. Commun.* **2011**, *47*, 5539−5541.

(42) Thordarson, P. *Chem. Soc. Rev.* **2011**, *40*, 1305−1323.

(43) Salis, A.; Ninham, B. W. *Chem. Soc. Rev.* **2014**, *43*, 7358−7377.

(44) Carnegie, R. S.; Gibb, C. L. D.; Gibb, B. C. *Angew. Chem., Int. Ed.* **2014**, *53*, 11498−11500.

(45) Gans, P.; Sabatini, A.; Vacca, A. *Talanta* **1996**, *43*, 1739−1753.

(46) Busschaert, N.; Bradberry, S. J.; Wenzel, M.; Haynes, C. J. E.; Hiscock, J. R.; Kirby, I. L.; Karagiannidis, L. E.; Moore, S. J.; Wells, N. J.; Herniman, J.; Langley, G. J.; Horton, P. N.; Light, M. E.; Marques, I.; Costa, P. J.; Felix, V.; Frey, J. G.; Gale, P. A. *Chem. Sci.* **2013**, *4*, 3036−3045.

(47) Lisbjerg, M.; Valkenier, H.; Jessen, B. M.; Al-Kerdi, H.; Davis, A. P.; Pittelkow, M. *J. Am. Chem. Soc.* **2015**, *137*, 4948−4951.

(48) Hammett analysis was also performed using the alternative parameters σ^+ and σ^- to better represent the build-up or depletion of charge; however, in all cases the fit was worse (Table S44). The build-up of charge is small in this case.

(49) Hancock, L. M.; Gilday, L. C.; Carvalho, S.; Costa, P. J.; Felix, V.; Serpell, C. J.; Kilah, N. L.; Beer, P. D. *Chem. - Eur. J.* **2010**, *16*, 13082−13094.